Electrochemical DNA Sensor

DOI: 10.1002/ange.201103482

Polarity-Switching Electrochemical Sensor for Specific Detection of Single-Nucleotide Mismatches**

Kuangwen Hsieh, Ryan J. White, Brian S. Ferguson, Kevin W. Plaxco, Yi Xiao, and H. Tom Soh**

Single-nucleotide polymorphisms (SNPs)—genetic variations that involve only a single DNA base-pair—can directly affect transcriptional regulations and protein functions.[1,2] Thus, SNP genotyping serves as an important diagnostic for genetic diseases[3–5] and drug responses.[6,7] To date, methods of detecting such single-nucleotide mismatches can be broadly categorized into enzyme-aided[8–13] and hybridization-based[14–16] approaches. The enzyme-aided approach typically involves a two-step, multi-component assay, in which a single-nucleotide-specific enzymatic reaction, such as primer extension,[8,9] ligation,[10,11] or cleavage,[12,13] is coupled with a downstream detection of reaction products. As such, these methods are inherently complex, and the assay specificity is limited by both the activity of the enzyme and the sensitivity of the detection technique. In contrast, hybridization-based methods utilize DNA probes[17–20] and various measurement techniques[17,21–23] to report the hybridization difference between perfectly matched (PM) and single-nucleotide mismatched (SM) targets in a single-step. However, to resolve the small difference in thermodynamic stability between the two targets, these detection methods generally require complex probe designs[18–20] and the careful control of hybridization conditions such as buffer composition,[14,16] washing stringency,[14,16] and melting temperature.[15]

In addition to these complex requirements, both enzyme-aided and hybridization-based approaches are susceptible to false-positives because they can only measure the difference in the signal amplitude between PM and SM targets—and signal amplitude measurements are prone to fluctuation in target/probe concentrations, background contaminants, and other experimental perturbations (e.g., enzyme activity, washing stringency or temperature). Thus, for robust detection of single-nucleotide mismatches, there is a need for alternative sensor architectures that are less prone to errors from fluctuations in the signal amplitude.

Toward this end, we present a single-step, room-temperature electrochemical sensor that detects single-nucleotide mismatches with a "polarity-switching" response. Our "bipolar" sensor reports a decreased output signal (signal-off) when hybridized with a PM target (Figure 1 a, top right) but reports an opposite, increased signal (signal-on) when hybridized with a SM target (Figure 1 a, bottom right). The output signal of the sensor is generated by the redox reporter methylene blue (MB), which is covalently attached to an electrode-bound DNA probe. The polarity-switching response is achieved by tuning two key parameters—the structural flexibility of the probe[24–28] and its interaction with the MB tag[29–40]—that control the electron transfer between the MB tag and the electrode. In this work, we describe the design principles of the bipolar sensor and demonstrate its performance in discriminating SM and PM targets under various conditions. Furthermore, we elucidate the mechanism behind the polarity-switching behavior and quantify the relative contributions of the two parameters that govern the sensor output.

The change in the output Faradaic current of our sensor is caused by alterations in the rate of electron transfer to the gold interrogating electrode, which is governed by the equilibrium probability of the DNA-bound MB tag approaching the electrode surface.[41] In our sensor design, we exploited the structural flexibility of the DNA probe[24,26–28] and the interaction between MB and DNA (e.g., intercalation and groove binding) to achieve mismatch detection through polarity switching. Regarding the probe flexibility parameter, the higher flexibility of single-stranded DNA (ssDNA) relative to rigid double-stranded DNA (dsDNA) increases the MB electron transfer rate and yields higher Faradaic currents.[24,26–28] In parallel, the interaction between the MB tag and dsDNA decreases the electron transfer rate, thus reducing the Faradaic current. This decreased electron transfer is presumably due to the confinement of the MB tag within the DNA duplex, which lowers the probability of the MB approaching the electrode.[40,41] Of note, this MB-dsDNA interaction depends on the DNA sequence,[29,39] which therefore needs to be evaluated prior to sensor design. In the present case, we have experimentally determined that the interaction between MB and poly(thymine–adenosine) (T-A) duplexes effectively slows MB electron transfer rate com-

[*] Dr. Y. Xiao, Prof. H. T. Soh
Materials Department, Department of Mechanical Engineering
University of California, Santa Barbara
Santa Barbara, CA 93106 (USA)
E-mail: yixiao@physics.ucsb.edu
tsoh@engr.ucsb.edu
K. Hsieh, Dr. B. S. Ferguson
Department of Mechanical Engineering
University of California, Santa Barbara (USA)
Dr. R. J. White, Prof. K. W. Plaxco
Department of Chemistry and Biochemistry
University of California, Santa Barbara (USA)

[**] We thank Seung Soo Oh for his assistance with fluorescence measurements, and Kareem Ahmad and Dr. Jonathan Adams for valuable discussions. This work is supported by Office of Naval Research, the National Institutes of Health, and ARO Institute for Collaborative Biotechnologies (ICB).

Supporting information (experimental section) for this article is available on the WWW under http://dx.doi.org/10.1002/anie.201103482.

© 2011 Wiley-VCH Verlag GmbH & Co. KGaA, Weinheim

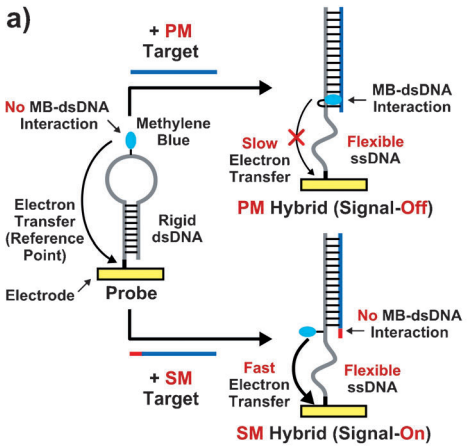

	Probe	PM Hybrid	SM Hybrid
Proximal End Flexibility	Rigid	Flexible	Flexible
MB-dsDNA Interaction	No	Yes	No
MB Electron Transfer	Reference Point	Slower than Reference	Faster than Reference
Sensor Signal Polarity		Signal-Off	Signal-On

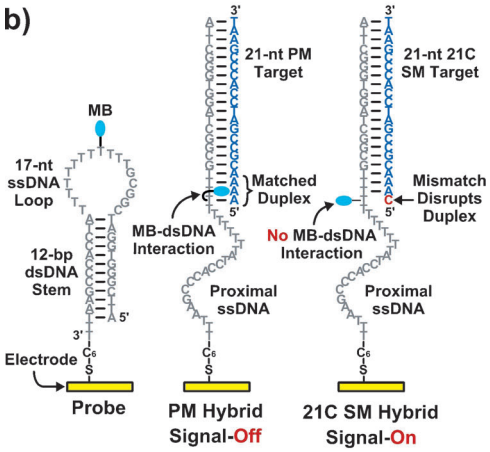

Figure 1. a) The bipolar sensor exploits the probe flexibility and the MB-dsDNA interaction to tune the electron transfer between the MB tag and the electrode, so that the sensor reports a "signal-off" response from the PM target, but an opposite "signal-on" response from the SM target. b) In the absence of target, the double-stranded stem of the probe creates proximal rigidity while the centrally-located MB does not interact with the single-stranded DNA loop. Upon target hybridization, both PM and SM target–probe hybrids are single-stranded at the proximal end, enhancing structural flexibility. In the PM hybrid the MB can interact with the double-stranded, poly-T-A region (center). The mismatched T-C bases in the SM hybrid disrupt this interaction (right), giving rise to the opposite signal polarity.

pared to related mismatches, and have exploited this finding for the sensor design.

Our insights in controlling these two parameters to tune the MB electron transfer have allowed us to rationally design a probe that specifically differentiates the PM target from the SM target with opposite signal polarities. Specifically, our probe consists of a 12-base-pair (bp) stem and a 17-nucleotide (nt) loop (Figure 1a, left; Figure 1b, left). The thiolated 3′ terminal is immobilized onto the gold electrode, and the MB molecule is modified onto a thymine base located at the center of the single-stranded loop. In the absence of target, the double-stranded stem creates proximal rigidity and the single-stranded loop prevents undesired MB-DNA interaction.[34] The high ionic strength of our high-salt phosphate buffer (HSPB) also effectively shields any electrostatic interaction between MB and DNA.[35,39] Subsequently, PM and SM target hybridization both displace the double-stranded stem and form target-probe hybrids that become single-stranded near the electrode. Although the structural flexibility is increased for both targets, only the PM target forms a T-A matched duplex that allows MB to interact with the dsDNA, presumably by groove binding to the poly-T-A region.[38] This decreases the rate of electron transfer, resulting in a signal-off response (Figure 1a, top right; Figure 1b, center). In contrast, the T-C mismatched bases in the SM target-probe hybrid disrupt MB-dsDNA interaction, increasing the rate of electron transfer and producing a signal-on response (Figure 1a, bottom right; Figure 1b, right). In this way, our sensor reports mismatches with an opposite signal polarity rather than differences in signal amplitude.

We experimentally verified the polarity-switching response of our sensor by challenging it with 21-nt PM and SM (5′ end-mismatched cytosine, denoted 21-nt 21C; Figure 1b, right) targets and measuring the sensor responses with alternating current voltammetry (ACV). In the absence of target, the sensor yielded an approximately 70 nA Faradaic redox peak current (Figure 2a, black), which served as the reference point. When challenged with the PM target (T-A match), we observed a signal-off behavior, with a 35% decrease in peak current (ca. 45 nA, Figure 2a, blue). Conversely, we detected a clear signal-on response from the 21-nt 21C SM target (T-C mismatch), displaying a 220% increase in the peak current with respect to the no-target signal (ca. 225 nA, Figure 2a, red).

We subsequently determined the optimal condition of the hybridization time, the ACV operating frequency, and the surface probe density to maximize the sensor performance. The sensor response was relatively rapid, as opposite signal polarities caused by the PM or the SM targets were observed within 10 min (Supporting Information, Figure S1). For typical experiments, however, we used a 2 h incubation time to saturate the sensor signal. Next, we optimized the ACV frequency[26,28] to obtain the greatest difference between the PM target and the SM target output responses. The sensor exhibited bipolar functionality between 1 to 20 Hz with a maximal differential output at 10 Hz, which was used throughout this work (Supporting Information, Figure S2). Finally, we found the optimal probe surface density by adjusting the probe concentration from 0.05 to 1.5 μM during sensor fabrication. We observed polarity-switching responses at all concentrations, and found that surface probe density of 1.62 ± 0.17 pmol cm^{-2} (fabricated with 0.5 μM of the probe) showed the best sensor response (Supporting Information, Figure S3a and S3b).[42–44]

To confirm the generality of the bipolar sensor, we characterized the sensor performance in detecting various SM targets containing different mismatches at the same position (Figure 2b). As expected, we observed reproducible signal-off responses from the 21-nt PM target (T-A match;

 © 2011 Wiley-VCH Verlag GmbH & Co. KGaA, Weinheim

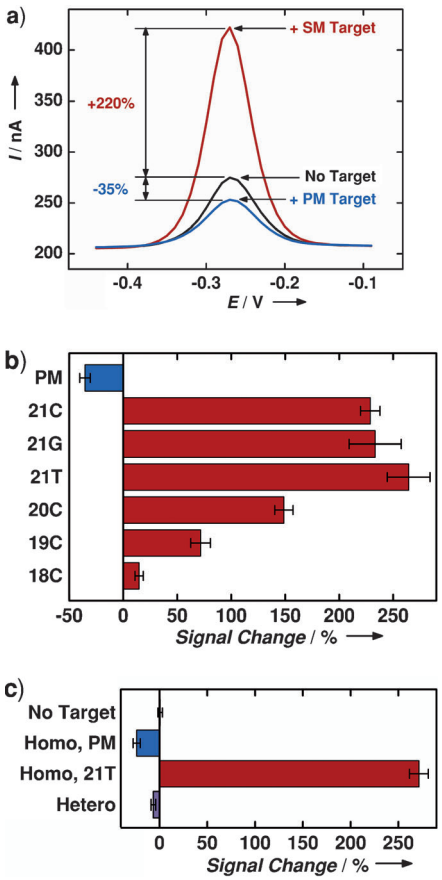

Figure 2. a) AC voltammograms show that relative to the no-target redox peak current (black), the sensor yields an decrease in the peak current (signal-off) when hybridized with the PM target (blue) but an increase in the peak current (signal-on) with a SM target (red). b) The sensor reports signal-on responses with similar magnitudes for all three mismatched bases at the fixed position (21-nt 21C, 21G, and 21T). The sensor maintains its signal-on response, when the position of the mismatched cytosine is moved stepwise from 21C to 18C. c) Sensor functionality in PCR mix: the sensor can differentiate background contaminants from the PCR mix (black), homozygous PM (blue), homozygous SM (red), and heterozygous mixture containing both PM and SM targets (purple). The values and error bars in this Figure and subsequent figures represent the mean and the standard deviation from triplicate measurements.

$-35.4 \pm 4.9\,\%$) and signal-on responses from 21-nt SM targets in which the mismatched base was guanine (21-nt 21G; T-G mismatch: $+233.3 \pm 24.1\,\%$), thymine (21-nt 21T; T-T mismatch: $+264.3 \pm 19.8\,\%$) or cytosine (21-nt 21C; T-C mismatch: $+228.8 \pm 9.0\,\%$), suggesting that the sensor discriminates all three mismatched bases equally well.

Next, we tested the sensor against mismatched bases at different positions within the 21-nt target. We fixed the mismatched base as cytosine, but moved the SM position stepwise from base 21 to base 18 in the 5′-to-3′ direction (i.e., 21-nt 21C to 21-nt 18C). While signal-on polarity remained consistent, the signal amplitude decreased as the mismatch position moved from 21C to 18C (Figure 2b). Compared to the signal from 21C SM target ($+228.8 \pm 9.0\,\%$), the 20C, 19C, and 18C SM targets yielded signal gains of $+148.78 \pm 8.4\,\%$, $+71.6 \pm 9.1\,\%$, and $+14.7 \pm 3.8\,\%$, respectively. This location-dependent signal decrease is due the fact that, as the mismatch moves further from the MB tag, the tag begins to interact with the duplex. This result indicates that the mismatch needs to be located within three nucleotides of the MB-modified thymine to preserve polarity-switching.

Importantly, we verified the sensor functionality in a complex mixture, and chose to do so in a polymerase chain reaction (PCR) mix because PCR is often utilized in clinical SNP detection assays. Without any targets, the bipolar sensor did not respond to the background contaminants in the PCR mix, and produced a minimal signal ($0.6 \pm 2.3\,\%$; Figure 2c, black). In the PCR mix, our sensor reported its signature polarity-switching responses for the PM and SM targets, producing a $-24.0 \pm 3.7\,\%$ PM response (21-nt, Figure 2c, blue) versus a $271.5 \pm 9.9\,\%$ SM response (21-nt 21T, Figure 2c, red), which are comparable to the measurements in buffer (Figure 2b).

In addition to the homozygous samples, which contain only either the PM targets or the SM targets, we also tested our sensor against a heterozygous mixture of 21-nt PM and 21-nt 21T SM targets at equal concentrations in the PCR mix. This heterozygous sample is representative of conditions where the mismatch occurs in only one of the two alleles. In this test, we measured a near-zero response of $-6.5 \pm 2.4\,\%$ (Figure 2c, purple). We note that this signal is clearly distinguishable from the sensor response to PM and SM targets and suggests that, in addition to the signal-on or signal-off responses, the sensor may be optimized to report a third state (zero-response state) for the detection of heterozygous samples.

To verify that our proposed electron transfer-based signaling mechanism is indeed responsible for the performance of our bipolar sensor, we performed two control experiments and show that, without the electrochemical signaling, the stem-loop probe structure cannot discriminate SM from PM targets. First, we directly hybridized our probe with PM (21-nt) and SM (21-nt 21C) targets in HSPB solution, and analyzed the hybridized products by gel electrophoresis. We observed that the PM and SM hybrid bands were equivalent in length and similar in band intensity, suggesting that both targets hybridize equally well to the probe (Supporting Information, Figure S3). In the second control experiment, we used a molecular beacon version of our probe, with a fluorophore-quencher pair located at the ends (CAL FLUOR RED 610 at the 5′-end and BHQ-2 at the 3′-end; DNA sequence shown in Supporting Information, Table S1). We then hybridized this modified molecular beacon with the PM and SM targets in HSPB and measured the fluorescence change. Both targets were able to completely open the molecular beacon probe, yielding similar intensity of fluorescence signal (Supporting Information Figure S4). These two experiments indicate that the stem-loop structure itself has minimal effect in differentiating mismatched bases and does not contribute to the polarity switching behavior. These results are consistent with the fact that the standard Gibbs free energy of the PM hybrid ($-46.34\,\mathrm{kcal\,mol^{-1}}$) closely matches that of the SM hybrid ($-44.39\,\mathrm{kcal\,mol^{-1}}$).

The output signal of our bipolar sensor is the net result of two signaling parameters—probe flexibility and MB-dsDNA

© 2011 Wiley-VCH Verlag GmbH & Co. KGaA, Weinheim

interaction. Thus, in order to determine the contribution of only the probe flexibility parameter to the sensor output, we had to minimize the contribution of MB-dsDNA interaction to the sensor output. For this evaluation, we employed two short targets in a two-step hybridization experiment that first increased the probe flexibility and then restored the original probe rigidity and measured the sensor responses of each step. Importantly, both short targets minimize the signaling contribution from MB-dsDNA interaction because the ends of the double-stranded elements in the resulting hybrid are located at least two nucleotides away from the MB tag, which is beyond the reach of the short C_6 linker that tethers the MB to the probe. We first challenged the probe (Figure 3a, left) with a 19-nt target that forms a proximally flexible target-probe hybrid (Figure 3a, center); subsequently, we challenged the hybrid with an additional 12-nt target complementary to the single-stranded element—analogous to reforming the original probe stem (Figure 3a, right). As expected, from the increased probe flexibility due to the first hybridization, the sensor reported a $246.7 \pm 19.9\%$ increase in redox peak current relative to the no-target signal (Figure 3a, center). When the original probe rigidity was restored by the second hybridization, the signal change diminished to a mere $12.2 \pm 1.5\%$ with respect to the no-target signal (Figure 3a, right). Thus, this two-step experiment clearly indicated that increased probe flexibility near the electrode was essential to increased output signal.

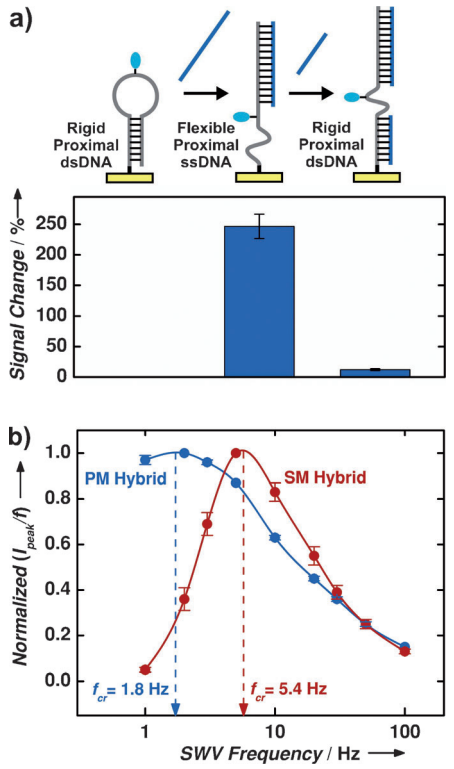

Figure 3. a) Increasing the probe flexibility by disrupting the stem increases the output signal (center). Restoring the rigidity of the stem returns the signal to its initial value (right). b) Plot of critical frequencies (f_{cr}) obtained from square-wave voltammetry (SWV) of 21-nt PM (blue) and 21-nt 21C SM (red) target–probe hybrids. The PM hybrid exhibits lower f_{cr}, indicating slow electron transfer.

Next, we minimized the contribution from the change in probe flexibility and evaluated the contribution from the MB-dsDNA interaction to the sensor output signal by comparing the difference in signal between 21-nt PM and 21-nt 21C SM targets using ACV and square-wave voltammetry (SWV) measurements. Due to the nearly identical structural flexibility of the two hybrids, differences in the output signal can be directly attributed to differences in the MB-dsDNA interaction. ACV measurements showed a large signal difference between the PM ($-35.4 \pm 4.9\%$) and SM ($+228.8 \pm 9.0\%$) targets (Figure 2b), clearly indicating the role of MB-dsDNA interaction in decreasing the output signal upon PM binding. To further support this observation, we measured the apparent MB electron transfer rates of the PM and SM hybrids with the SWV technique.[28,45,46] We used the critical frequency (f_{cr})[46] (defined as the frequency at which the maximal value of SWV frequency-normalized peak current (I_{peak}/f) is observed) of each hybrid to quantify electron transfer between MB and electrode. Since f_{cr} is linearly proportional to the transfer rate, a smaller f_{cr} represents slower electron transfer. We obtained a f_{cr} of approximately 1.8 Hz for the PM hybrid (Figure 3b, blue) versus approximately 5.4 Hz for the SM hybrid (Figure 3b, red), suggesting that the MB-dsDNA interaction in the PM hybrid reduces the apparent MB electron transfer rate by a factor of approximately 3, giving rise to the decreased sensor signal.

We recombined the two parameters to evaluate the net signaling effect and identify the point at which the output signal switches polarity. We measured the output from four PM targets of increasing length (19- to 22-nt; Figure 4). We note that the proximal end of each target-probe hybrid is single-stranded and flexible; however, the MB-dsDNA interaction becomes stronger as the target is lengthened. For example, for the 19-nt target, we found that probe flexibility dominates the output signal because the end of the hybrid is located two nucleotides away from the MB molecule,

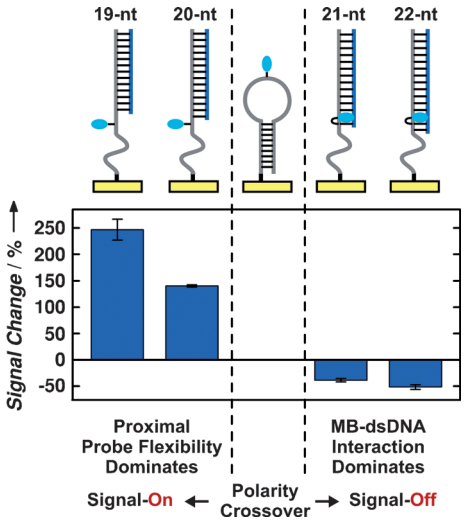

Figure 4. Using PM targets of increasing length (19- to 22-nt), the point at which the output signal changes its polarity can be identified. This point is where the MB-dsDNA interaction begins to dominate the output signal.

© 2011 Wiley-VCH Verlag GmbH & Co. KGaA, Weinheim

minimizing its MB-dsDNA interaction. When the target was lengthened from 20- to 21-nt, we observed a switch in the response from signal-on ($+140.3 \pm 2.2\,\%$) to signal-off ($-35.4 \pm 4.9\,\%$). This signal crossover represents the point at which the influence of the MB-dsDNA interaction begins to dominate over the probe flexibility. This polarity crossover closely matched the responses observed with PM and SM targets. From these observations, we conclude that increased probe flexibility is a prerequisite to the polarity-switching responses; however, the crossover point is dependent on the strength of the MB-dsDNA interaction.

In summary, we report a single-step, room-temperature electrochemical sensor that identifies single-nucleotide mismatches with a polarity-switching output. Compared to previous detection methods, our bipolar sensor offers simplicity and robustness because it reports the mismatch with a switch in its signal polarity, rather than differences in its signal amplitude, which are prone to false-positives. This important feature is obtained by tuning the probe structural flexibility and the strength of the interaction between MB and double-stranded DNA. Specifically, we observe that increased flexibility in the proximal end of the DNA probe increases the sensor signal, whereas strong interactions between MB and double-stranded DNA slow down electron transfer, yielding a decreased output signal. We found that the polarity-switching responses are independent of mismatch base substitutions, but begin to diminish as the mismatch location is moved away from the DNA-bound MB redox reporter, and we identified the crossover point at which the output signal changes its polarity. Furthermore, we show that the operation of our bipolar sensor in complex mixtures such as PCR mixes does not affect its performance. With further optimization of the probe design, as well as the integration with clinical sample processing, we believe our bipolar sensor platform may provide an alternative strategy for rapid and robust SNP genotyping.

Received: May 20, 2011
Revised: August 19, 2011
Published online: October 4, 2011

Keywords: DNA · electrochemistry · sensors · single-nucleotide mismatch

[1] S. Kim, A. Misra, *Annu. Rev. Biomed. Eng.* **2007**, *9*, 289.
[2] R. M. Bertina, B. P. C. Koeleman, T. Koster, F. R. Rosendaal, R. J. Dirven, H. Deronde, P. A. Vandervelden, P. H. Reitsma, *Nature* **1994**, *369*, 64.
[3] S. L. Naylor, *Front. Biosci.* **2007**, *12*, 4111.
[4] Y. Suh, J. Vijg, *Mutat. Res. Fundam. Mol. Mech. Mutagen.* **2005**, *573*, 41.
[5] A. J. Schafer, J. R. Hawkins, *Nat. Biotechnol.* **1998**, *16*, 33.
[6] W. E. Evans, M. V. Relling, *Science* **1999**, *286*, 487.
[7] J. J. McCarthy, R. Hilfiker, *Nat. Biotechnol.* **2000**, *18*, 505.
[8] B. P. Sokolov, *Nucleic Acids Res.* **1990**, *18*, 3671.
[9] T. T. Nikiforov, R. B. Rendle, P. Goelet, Y. H. Rogers, M. L. Kotewicz, S. Anderson, G. L. Trainor, M. R. Knapp, *Nucleic Acids Res.* **1994**, *22*, 4167.
[10] D. A. Nickerson, R. Kaiser, S. Lappin, J. Stewart, L. Hood, U. Landegren, *Proc. Natl. Acad. Sci. USA* **1990**, *87*, 8923.
[11] U. Landegren, R. Kaiser, J. Sanders, L. Hood, *Science* **1988**, *241*, 1077.
[12] D. Botstein, R. L. White, M. Skolnick, R. W. Davis, *Am. J. Hum. Genet.* **1980**, *32*, 314.
[13] V. Lyamichev, A. L. Mast, J. G. Hall, J. R. Prudent, M. W. Kaiser, T. Takova, R. W. Kwiatkowski, T. J. Sander, M. de Arruda, D. A. Arco, B. P. Neri, M. A. D. Brow, *Nat. Biotechnol.* **1999**, *17*, 292.
[14] R. K. Saiki, P. S. Walsh, C. H. Levenson, H. A. Erlich, *Proc. Natl. Acad. Sci. USA* **1989**, *86*, 6230.
[15] W. M. Howell, M. Jobs, U. Gyllensten, A. J. Brookes, *Nat. Biotechnol.* **1999**, *17*, 87.
[16] G. C. Kennedy, H. Matsuzaki, S. L. Dong, W. M. Liu, J. Huang, G. Y. Liu, X. Xu, M. Q. Cao, W. W. Chen, J. Zhang, W. W. Liu, G. Yang, X. J. Di, T. Ryder, Z. J. He, U. Surti, M. S. Phillips, M. T. Boyce-Jacino, S. P. A. Fodor, K. W. Jones, *Nat. Biotechnol.* **2003**, *21*, 1233.
[17] S. Tyagi, F. R. Kramer, *Nat. Biotechnol.* **1996**, *14*, 303.
[18] D. M. Kolpashchikov, *J. Am. Chem. Soc.* **2006**, *128*, 10625.
[19] Y. Xiao, X. G. Qu, K. W. Plaxco, A. J. Heeger, *J. Am. Chem. Soc.* **2007**, *129*, 11896.
[20] Y. Xiao, K. J. I. Plakos, X. H. Lou, R. J. White, J. R. Qian, K. W. Plaxco, H. T. Soh, *Angew. Chem.* **2009**, *121*, 4418; *Angew. Chem. Int. Ed.* **2009**, *48*, 4354.
[21] P. M. Diakowski, H. B. Kraatz, *Chem. Commun.* **2009**, 1189.
[22] R. Ikeda, S. Kobayashi, J. Chiba, M. Inouye, *Chem. Eur. J.* **2009**, *15*, 4822.
[23] Y. Wang, C. Li, X. Li, Y. Li, H.-B. Kraatz, *Anal. Chem.* **2008**, *80*, 2255.
[24] A. Anne, C. Demaille, *J. Am. Chem. Soc.* **2006**, *128*, 542.
[25] A. Anne, C. Demaille, *J. Am. Chem. Soc.* **2008**, *130*, 9812.
[26] F. Ricci, R. Y. Lai, A. J. Heeger, K. W. Plaxco, J. J. Sumner, *Langmuir* **2007**, *23*, 6827.
[27] F. Ricci, R. Y. Lai, K. W. Plaxco, *Chem. Commun.* **2007**, 3768.
[28] R. J. White, K. W. Plaxco, *Anal. Chem.* **2010**, *82*, 73.
[29] E. Tuite, B. Norden, *J. Am. Chem. Soc.* **1994**, *116*, 7548.
[30] E. Tuite, J. M. Kelly, *Biopolymers* **1995**, *35*, 419.
[31] S. O. Kelley, J. K. Barton, N. M. Jackson, M. G. Hill, *Bioconjugate Chem.* **1997**, *8*, 31.
[32] A. Erdem, K. Kerman, B. Meric, U. S. Akarca, M. Ozsoz, *Anal. Chim. Acta* **2000**, *422*, 139.
[33] R. Rohs, H. Sklenar, R. Lavery, B. Roder, *J. Am. Chem. Soc.* **2000**, *122*, 2860.
[34] A. Tani, A. J. Thomson, J. N. Butt, *Analyst* **2001**, *126*, 1756.
[35] P. Kara, K. Kerman, D. Ozkan, B. Meric, A. Erdem, Z. Ozkan, M. Ozsoz, *Electrochem. Commun.* **2002**, *4*, 705.
[36] E. M. Boon, N. M. Jackson, M. D. Wightman, S. O. Kelley, M. G. Hill, J. K. Barton, *J. Phys. Chem. B* **2003**, *107*, 11805.
[37] H. C. M. Yau, H. L. Chan, M. S. Yang, *Biosens. Bioelectron.* **2003**, *18*, 873.
[38] R. Rohs, H. Sklenar, *J. Biomol. Struct. Dyn.* **2004**, *21*, 699.
[39] M. Hossain, G. S. Kumar, *Mol. BioSyst.* **2009**, *5*, 1311.
[40] A. A. Lubin, B. V. S. Hunt, R. J. White, K. W. Plaxco, *Anal. Chem.* **2009**, *81*, 2150.
[41] T. Uzawa, R. R. Cheng, R. J. White, D. E. Makarov, K. W. Plaxco, *J. Am. Chem. Soc.* **2010**, *132*, 16120.
[42] S. E. Creager, T. T. Wooster, *Anal. Chem.* **1998**, *70*, 4257.
[43] S. D. O'Connor, G. T. Olsen, S. E. Creager, *J. Electroanal. Chem.* **1999**, *466*, 197.
[44] J. J. Sumner, K. S. Weber, L. A. Hockett, S. E. Creager, *J. Phys. Chem. B* **2000**, *104*, 7449.
[45] S. Komorsky-Lovrić, M. Lovric, *J. Electroanal. Chem.* **1995**, *384*, 115.
[46] S. Komorsky-Lovrić, M. Lovric, *Anal. Chim. Acta* **1995**, *305*, 248.

© 2011 Wiley-VCH Verlag GmbH & Co. KGaA, Weinheim